Stimulated Brillouin scattering of visible light in small-core photonic crystal fibers

R. I. Woodward, E. J. R. Kelleher, S. V. Popov, and J. R. Taylor

Femtosecond Optics Group, Department of Physics, Imperial College London, Prince Consort Road, London SW7 2BW, UK
Corresponding author: r.woodward12@imperial.ac.uk

Received November 29, 2013; revised March 11, 2014; accepted March 11, 2014;
posted March 12, 2014 (Doc. ID 202293); published April 8, 2014

We characterize stimulated Brillouin scattering (SBS) of visible light in small-core photonic crystal fiber (PCF). Threshold powers under 532 nm excitation agree with established theory, in contrast to measured values up to five times greater than expected for Brillouin scattering of 1550 nm light. An isolated, single-peaked signal at a Stokes shift of 33.5 GHz is observed, distinct from the multi-peaked Stokes spectra expected when small-core PCF is pumped in the infrared. This wavelength-dependence of the Brillouin threshold, and the corresponding spectrum, are explained by the acousto-optic interactions in the fiber, governed by dimensionless length scales that relate the modal area to the core size, and the pump wavelength to PCF hole pitch. Our results suggest new opportunities for exploiting SBS of visible light in small-core PCFs.

OCIS codes: (060.4005) Microstructured fibers; (060.4370) Nonlinear optics, fibers; (060.5295) Photonic crystal fibers; (290.5900) Scattering, stimulated Brillouin.
http://dx.doi.org/10.1364/OL.39.002330

Stimulated Brillouin scattering (SBS) is a nonlinear optical effect that is facilitating the development of new laser sources, distributed fiber sensors, and slow-light devices. A low SBS threshold power is desirable, minimizing the pump power required to achieve significant backscattering of light from acousto-optic interactions in the fiber. Photonic crystal fibers (PCFs) with a small core are a promising medium for exploiting SBS, since the enhancement of effective nonlinearity through tighter confinement of the guided optical mode could increase the Brillouin gain, lowering the threshold power.

The magnitude and shape of the Brillouin gain spectrum depends on the overlap between acoustic and optical modes, which is strongly influenced by fiber geometry [1,2]. Acoustic modes can contain both longitudinal-wave and shear-wave components, although the longitudinal component dominates the Brillouin response [2]. In conventional step-index fiber the small acoustic impedance mismatch between core and cladding materials results in weak reflections at their interface and minimal coupling between longitudinal and shear waves. Consequently, the acoustic waves generated through electrostriction are purely longitudinal waves resulting in strong Bragg backscattering of light and a single Brillouin peak [2,3].

PCFs with a small silica core exhibit a more complex Brillouin response due to richer acoustic dynamics. The air–glass boundaries result in strong reflections and coupling between longitudinal and shear acoustic waves [2]. The resulting hybrid modes exhibit different acoustic velocities and can give different Stokes shifts [2]. Therefore, multiple peaks have been observed in both spontaneous [2,4,5] and stimulated [6,7] Brillouin spectra. Dainese *et al.* also reported the evolution of the backscattered signal spectrum, with more peaks forming as the pump power increased, attributed to parametric mixing [2]. The more complex acoustic dynamics in small-core PCFs can lead to an increased SBS threshold. Thresholds up to a factor of five higher than predicted by theory have been reported [2,4–6], which have been explained by a reduced overlap between acoustic and optical modes [6], the increased shear strain content in acoustic modes that has a minimal contribution to SBS [2], and also due to structural variations along the PCF [5]. This higher threshold could suggest that PCFs offer little benefit over conventional step-index fiber for Brillouin scattering applications, although to date, studies of SBS in PCF have been restricted to infrared wavelengths.

In this Letter, we characterize SBS in a small-core PCF pumped with 532 nm light, without observing the widely reported increase in threshold and multi-peaked Stokes spectra. We verify these observations in a second small-core PCF and compare the Brillouin response to 532 and 1550 nm light, confirming the expected threshold increase and asymmetric Brillouin spectrum at 1550 nm. An explanation is proposed based on the relative size of the optical mode area to core size, and the wavelength to hole pitch. This is supported by numerical modeling to compute the fully vectorial core-confined eigenmodes of Maxwell's equations from a scanning electron microscope (SEM) image of the PCF microstructure [8].

Our experimental setup is shown in Fig. 1. Pump light at 532 nm with a linear polarization state was provided by a single-frequency continuous-wave frequency-doubled ytterbium-doped fiber laser (15 MHz linewidth). Power was controlled with a variable optical attenuator formed from a half-wave plate (HWP) and polarizer. Light was

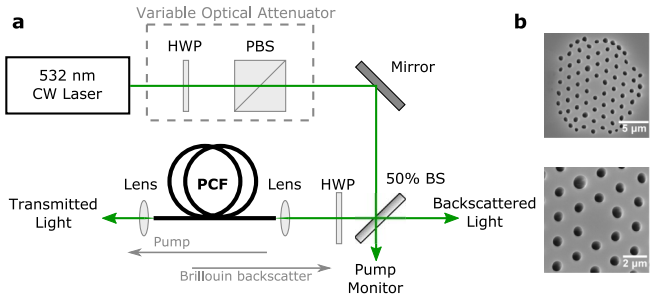

Fig. 1. (a) Setup: HWP, half-wave plate; (P)BS, (polarizing) beam splitter. (b) SEM images of PCF-1 microstructure at different magnifications.

launched into the PCF (55% coupling efficiency) through a second HWP, which was rotated to alter the polarization direction. The PCF, hereafter referred to as PCF-1, was 10 m long and endlessly single-moded, with core diameter $d_c = 3.0$ μm, air-hole pitch $\Lambda = 1.9$ μm, and hole diameter $d = 0.7$ μm [Fig. 1(b)]. A 50% beam splitter enabled monitoring of the backscattered signal. The output end of the fiber was angle-cleaved to eliminate feedback from Fresnel reflections and the polarization of backscattered signal was measured and corrections applied for the small polarization dependence of the beam splitter.

Initially, the linear pump polarization was aligned with a principal axis of the PCF. Characteristic SBS behavior was observed: the transmitted power increased linearly with increasing pump power until a threshold was reached, after which the transmitted power saturated and the backscattered signal increased sharply [Fig. 2(a)]. The threshold—defined as the pump power for which the backscattered signal is 1% of the input power—was measured as 220 mW. Similar results were obtained when the input polarization was rotated through 90° to align with the other principal axis of the fiber; although, when aligning the polarization between the two fiber axes (~45° rotation), the threshold and saturated transmitted power were approximately doubled. Such behavior is typical of a strongly birefringent fiber [9], and not a sixfold symmetric PCF microstructure which should not exhibit birefringence [10]. The apparent strong birefringence in PCF-1 is attributed to asymmetry from structural imperfections in the PCF structure, which can be seen in the SEM cross-sectional image [Fig. 1(b)] [7]. We further examined the Brillouin gain dependence on the input polarization angle (0°, defined as along a fiber principal axis) by rotating the HWP [Fig. 2(b)]. A sinusoidal variation in backscattered and transmitted powers was seen above threshold, due to the polarization dependence of Brillouin gain [9], and below threshold the transmission was independent of polarization, indicating no polarization-dependent loss.

The SBS threshold is given by [11]

$$P_{\text{th}} = \frac{21KA_{\text{eff}}}{g_B L_{\text{eff}}}, \tag{1}$$

where A_{eff} is the optical mode effective area, L_{eff} is the effective fiber length, $L_{\text{eff}} = (1 - e^{-\alpha L})/\alpha$ to account for loss α in a physical fiber length L, and g_B is the peak Brillouin gain. K is a polarization-dependent factor: $K = 1$ when the pump is coupled into a principal axis of strongly birefringent fiber, and $K = 2$ when launched at 45° to an axis [9]. For PCF-1, we measured a loss value of 61 dB/km from cut-back measurements and a value of $A_{\text{eff}} = 4.73$ μm^2 was extracted from modeling. Using these properties and our recorded threshold values, the peak Brillouin gain was calculated to be 4.8×10^{-11} m/W, in agreement with values typical of silica fibers [1]. The backscattered signal was also observed using a CCD camera, showing that it propagates as a fundamental core mode (Fig. 3 inset).

Stimulated backscattered light is Stokes shifted from the pump wavelength λ_p by: $f_{\text{SBS}} = 2n_{\text{eff}}v_A/\lambda_p$, where

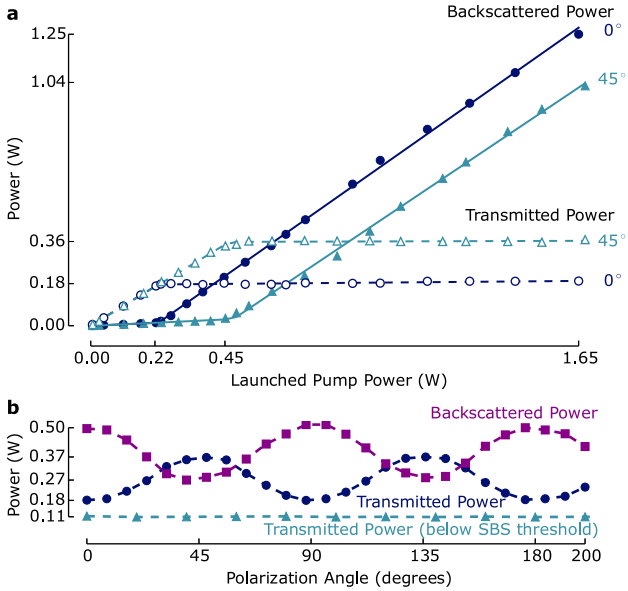

Fig. 2. Backscattered and transmitted powers in PCF-1 as a function of launched pump power (a) and input polarization angle (b). The highest Brillouin gain was observed for light aligned along a fiber principal axis (0°), approximately double the value for light polarized between axes (45°).

n_{eff} is the effective refractive index and v_A is the acoustic mode velocity [1]. We measured this shift using a scanning Fabry–Perot interferometer, monitoring the back-reflected light containing both Brillouin backscattered light and Fresnel-reflected pump light from the fiber front face. With an interferometer free-spectral range (FSR) of 42.2 GHz, we recorded a Brillouin shift of 33.5 ± 1.0 GHz (Fig. 3 top inset). Using $n_{\text{eff}} = 1.456$, as extracted from simulations, the measured shift relates to an acoustic velocity of ~6100±200 m/s, corresponding reasonably well to the known longitudinal acoustic velocity in silica of 5960 m/s [1]. The shape of the Stokes signal (Fig. 3) was measured by reducing the etalon FSR to 2.9 GHz with 50 MHz resolution (limited by interferometer finesse). While the measured Stokes peak width of 50 MHz was resolution-limited, we observed no asymmetry or multipeak structure.

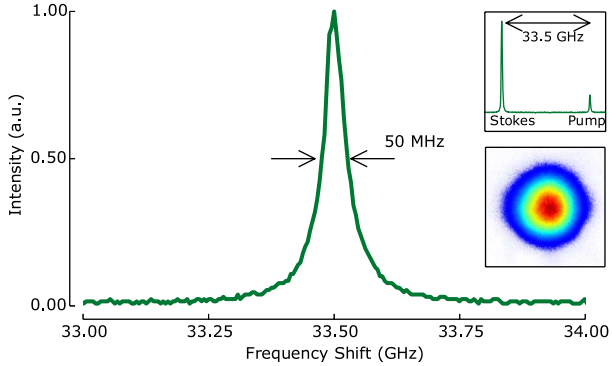

Fig. 3. Brillouin backscattered spectrum in PCF-1 from a scanning interferometer with 2.9 GHz FSR (top inset: with 42.2 GHz FSR, showing the Brillouin shift from the pump) for 0.5 W launched pump power aligned to a PCF principal axis. Bottom inset: output beam profile from a CCD camera.

The observation of an isolated single Stokes peak and the agreement between measured and theoretical threshold power at 532 nm are distinct from recent reports of Brillouin scattering measurements in small-core PCF at ~1550 nm [2,4–7]. SBS could not be observed in PCF-1 at 1550 nm for comparison, due to high confinement loss in the fiber at longer wavelengths. Therefore, to verify these observations, we characterized SBS in a second 40-m long PCF with a similar microstructure (PCF-2: $d_c = 2.3$ μm, $d = 0.55$ μm, and $\Lambda = 1.48$ μm; see Fig. 4 insets) but with more layers of air holes to reduce the confinement loss. The experiment was repeated with the 532 nm pump source (56% coupling efficiency into PCF-2) and also with a 1550 nm pump laser (1 MHz linewidth, 50% coupling efficiency). PCF-2's microstructure appears more symmetric and the pump polarization angle was found to have minimal effect on the Brillouin gain. This behavior is typical of a low birefringence fiber, for which a factor of $K = 3/2$ should be used in threshold calculations [9]. The measured loss at each wavelength and the effective area and effective index values obtained from modeling are shown in Table 1. From Eq. (1), the predicted threshold values are 70 and 240 mW at 532 and 1550 nm, respectively, (while the peak Brillouin gain is independent of wavelength [1], the effective area and loss are greater at 1550 nm, leading to a higher SBS threshold). Experimentally we measured threshold values of 69 mW at 532 nm and 1.16 W at 1550 nm. At 532 nm there is strong agreement between theory and the measured threshold power; however, at 1550 nm, the experimental value is ~5 times higher than predicted.

The spectral shape and frequency shift of the Stokes component at 532 and 1550 nm in the SBS regime (recorded with the interferometer) are shown in Fig. 4(a). The 11.0 ± 0.4 GHz Stokes shift measured at 1550 nm corresponds to an acoustic velocity of ~6050±175 m/s and the 33.4 ± 1.0 GHz shift at 532 nm gives a velocity of ~6110±200 m/s, both in agreement with the known velocity in silica [1]. The Brillouin signal at 532 nm is a symmetric single peak showing no substructure, similar to the shape observed with PCF-1. In contrast, the Stokes peak at 1550 nm shows strong asymmetry. While the limited resolution and sensitivity of our scanning interferometer prohibits a detailed analysis of the structure and acoustic mode content, the asymmetry at 1550 nm suggests interaction between the optical field and numerous acoustic modes, which each give slightly different frequency shifts. These observations support reports in literature of multi-peaked and high-threshold SBS behavior in small-core PCFs at 1550 nm, whereas at a pump wavelength of 532 nm we saw no such irregularity.

Acousto-optic dynamics in fiber can be determined by dimensionless length scales: Λ/λ and $A_{\text{eff}}/A_{\text{core}}$, with the effective optical mode area A_{eff} defined as [1]

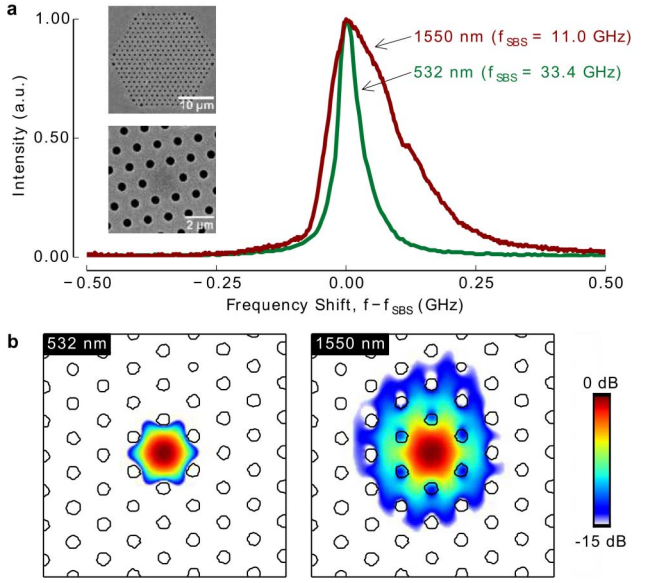

Fig. 4. (a) Brillouin backscattered spectra in PCF-2 for 532 and 1550 nm pump light showing strong asymmetry at 1550 nm (inset: SEM images of PCF-2 microstructure). (b) electric field densities of the fundamental mode, showing much weaker core-confinement at 1550 nm than at 532 nm.

$$A_{\text{eff}} = \frac{\left(\iint |E(x,y)|^2 \mathrm{d}x\mathrm{d}y\right)^2}{\int |E(x,y)|^4 \mathrm{d}x\mathrm{d}y}, \tag{2}$$

where $E(x,y)$ is the wavelength-dependent electric field distribution of the guided optical mode, and the physical core area is $A_{\text{core}} = \pi d_c^2/4$ (= 4.15 μm² in PCF-2). Additionally, we note that acoustic waves can spread out inside the fiber by diffraction. Comparing the acoustic diffraction length $l_d = A_{\text{core}}/\lambda_s$, where $\lambda_s = \lambda_p/2n_{\text{eff}}$ is the acoustic wavelength, to the sound attenuation length $l_a = v_A T_A$, where T_A is the acoustic lifetime, the diffraction efficiency is related to $l_a/l_d = \lambda_p v_A T_A/2n_{\text{eff}}A_{\text{core}}$ [12].

At 532 nm, $A_{\text{eff}} < A_{\text{core}}$ suggesting tight confinement of the optical mode, as verified by the computed mode profile [Fig. 4(b)]. The resulting overlap between acoustic waves in the cladding and the optical field is minimal, limiting Brillouin backscattering from cladding waves. Acoustic waves are formed in the core with predominantly longitudinal strain, generating strong Bragg gratings to backscatter pump light into Stokes light.

At 1550 nm, the optical field leaks into the cladding, since $A_{\text{eff}} > A_{\text{core}}$, suggesting interaction with acoustic cladding waves. Additionally, the diffraction efficiency depends on λ_p and T_A (which increases with λ_p) so the spreading of acoustic strains outward from the core at 1550 nm will be more than 3 times greater than at

Table 1. PCF-2 Properties at 532 and 1550 nm

					Threshold Power (mW)	
λ (nm)	Λ/λ	A_{eff} (μm²)	n_{eff}	α (dB/km)	Theory	Experiment
532	2.79	3.53	1.45	44	70	69
1550	0.96	7.87	1.41	153	240	1160

532 nm. Hence, there will be more reflections at the "hard" glass–air boundaries which couple longitudinal and shear waves. This results in numerous acoustic modes which give different frequency shifts and have significant shear components, forming multi-peaked backscattered spectra and reducing the Brillouin gain [2]. The air-hole cladding layer can also act as a resonant cavity to directly modulate backscattered light, imposing further peaks on the backscattered spectrum [3,6]. The multiple peaks that are expected in the Stokes spectrum appear as an asymmetric shape in our scanning interferometer trace [Fig. 4(a)] due to the limited measurement resolution. As light cannot be completely concentrated in the silica if $\lambda > \Lambda$, the pump field overlaps air holes, which further reduces the gain since these regions do not contribute to SBS. The reduced Brillouin gain at 1550 nm raises the SBS threshold, as confirmed by our observations. We note similarities between our conclusions and studies considering SBS of infrared light in large core PCFs, since both situations yield similar Λ/λ and $A_{\text{eff}}/A_{\text{core}}$ ratios [2,6].

While many reports to date have suggested that the enhanced nonlinearity in small-core PCFs is negated by complex acoustic dynamics, raising the SBS threshold, we believe that PCF does offer advantages over conventional step-index fiber for exploiting SBS if shorter wavelength pump light is used. Using the threshold power-effective length product, $P_{\text{th}}L_{\text{eff}}$ as a figure of merit, we find: conventional step-index fiber with $A_{\text{eff}} = 30\ \mu\text{m}^2$ and $\alpha = 0.2$ dB/km gives an estimate of $P_{\text{th}}L_{\text{eff}} = 19.7\ \text{W} \cdot \text{m}$ (approximately wavelength independent [1]); PCF-2 pumped with 1550 nm light exhibited $P_{\text{th}}L_{\text{eff}} = 25.1\ \text{W} \cdot \text{m}$; PCF-2 pumped with 532 nm light exhibited $P_{\text{th}}L_{\text{eff}} = 2.3\ \text{W} \cdot \text{m}$. These values show that, for an arbitrary length of fiber, the SBS threshold in small-core PCF pumped at 1550 m will exceed the threshold in a step-index fiber, although by using a 532 nm pump source with the same PCF, the threshold can be reduced by nearly an order of magnitude.

In summary, we have characterized SBS of visible light in small-core PCF and observed an SBS threshold power-effective length product an order of magnitude lower than pumping with infrared light. The single-peak Stokes spectrum, and the reduced threshold agree with established theory, but contrast earlier reports of Brillouin scattering in small-core PCF under 1550 nm excitation, where a more complex phonon interaction explains a multi-peaked Stokes emission and a factor of five increase of the SBS threshold. Enhanced confinement of the optical mode increases the interaction with longitudinal acoustic waves, leading to stronger SBS. Tighter modal confinement can be achieved using a shorter excitation wavelength, providing the opportunity to realize SBS-based devices with greatly reduced thresholds and higher efficiencies.

References

1. G. P. Agrawal, *Nonlinear Fiber Optics*, 5th ed. (Academic, 2013).
2. P. Dainese, P. St. J. Russell, N. Joly, J. C. Knight, G. S. Wiederhecker, H. L. Fragnito, V. Laude, and A. Khelif, Nat. Phys. **2**, 388 (2006).
3. I. Bongrand, É. Picholle, and C. Montes, Eur. Phys. J. D **20**, 121 (2002).
4. J.-C. Beugnot, T. Sylvestre, D. Alasia, H. Maillotte, V. Laude, A. Monteville, L. Provino, N. Traynor, S. F. Mafang, and L. Thévenaz, Opt. Express **15**, 15517 (2007).
5. J. H. Lee, Z. Yusoff, W. Belardi, M. Ibsen, T. M. Monro, and D. J. Richardson, Opt. Lett. **27**, 927 (2002).
6. J. E. McElhenny, R. K. Pattnaik, J. Toulouse, K. Saitoh, and M. Koshiba, J. Opt. Soc. Am. B **25**, 582 (2008).
7. J. E. McElhenny, R. Pattnaik, and J. Toulouse, J. Opt. Soc. Am. B **25**, 2107 (2008).
8. S. G. Johnson and J. D. Joannopoulos, Opt. Express **8**, 173 (2001).
9. M. O. van Deventer and A. J. Boot, J. Lightwave Technol. **12**, 585 (1994).
10. M. J. Steel, T. P. White, C. M. de Sterke, R. C. McPhedran, and L. C. Botten, Opt. Lett. **26**, 488 (2001).
11. R. G. Smith, Appl. Opt. **11**, 2489 (1972).
12. B. Y. Zel'dovich and A. N. Pilipetskii, Sov. J Quantum Electron. **16**, 546 (1986).